Science AAAS

Marine Radiocarbon Evidence for the Mechanism of Deglacial Atmospheric CO_2 Rise

Thomas M. Marchitto, *et al.*

Science **316**, 1456 (2007);
DOI: 10.1126/science.1138679

28. D. King, J. Roughgarden, *Theor. Popul. Biol.* **21**, 194 (1982).
29. D. Cohen, *J. Theor. Biol.* **12**, 119 (1966).
30. D. King, J. Roughgarden, *Theor. Popul. Biol.* **22**, 1 (1982).
31. P. Haccou, Y. Iwasa, *Theor. Popul. Biol.* **47**, 212 (1995).
32. E. Kussell, S. Leibler, *Science* **309**, 2075 (2005).
33. L. Watson, M. J. Dallwitz, *The Families of Flowering Plants: Descriptions, Illustrations, Identification, and Information Retrieval.* Version: 29 July 2006 http://delta-intkey.com (1992 onward).
34. T. Keller, J. Abbott, T. Moritz, P. Doerner, *Plant Cell* **18**, 598 (2006).
35. A. C. Whibley *et al.*, *Science* **313**, 963 (2006).
36. S. Gavrilets, *Fitness Landscapes and the Origin of Species*, S. Levin, H. Horn, Eds., Monographs in Population Biology (Princeton Univ. Press, Princeton and Oxford, 2004).

37. We thank J. Avondo for help with visualizing 3D fitness landscapes, M. Clauss for helpful discussions on bet-hedging, and C. Thébaud for advice on inflorescence databases. This research was funded by grants from Human Frontier Science Program (E.C. and P.P.), Natural Sciences and Engineering Research Council of Canada (P.P. and L.H.), and the Biotechnology and Biological Sciences Research Council, UK (E.C.).

Supporting Online Material
www.sciencemag.org/cgi/content/full/1140429/DC1
Materials and Methods
SOM Text
Fig. S1
References
SOM Programs

25 January 2007; accepted 30 April 2007
Published online 24 May 2007;
10.1126/science.1140429
Include this information when citing this paper.

Marine Radiocarbon Evidence for the Mechanism of Deglacial Atmospheric CO_2 Rise

Thomas M. Marchitto,[1,2]*† Scott J. Lehman,[1,2]* Joseph D. Ortiz,[3] Jacqueline Flückiger,[2]‡ Alexander van Geen[4]

We reconstructed the radiocarbon activity of intermediate waters in the eastern North Pacific over the past 38,000 years. Radiocarbon activity paralleled that of the atmosphere, except during deglaciation, when intermediate-water values fell by more than 300 per mil. Such a large decrease requires a deglacial injection of very old waters from a deep-ocean carbon reservoir that was previously well isolated from the atmosphere. The timing of intermediate-water radiocarbon depletion closely matches that of atmospheric carbon dioxide rise and effectively traces the redistribution of carbon from the deep ocean to the atmosphere during deglaciation.

Radiocarbon measurements of calendrically dated hermatypic corals (*1*) and planktonic foraminifera (*2*, *3*) indicate that the radiocarbon activity ($\Delta^{14}C$) of the atmosphere during the latter part of the last glacial period [~20,000 to 40,000 years before the present (yr B.P.)] ranged from ~300 to 800 per mil (‰) higher than it was during the prenuclear modern era (Fig. 1C). Although reconstructions of Earth's geomagnetic-field intensity predict higher cosmogenic ^{14}C production rates during the glacial period, production was apparently not high enough to explain the observed atmospheric enrichment (*2*–*5*). Rather, a substantial fraction of the atmosphere's $\Delta^{14}C$ buildup must have been due to decreased uptake of ^{14}C by the deep ocean. This requires a concomitant ^{14}C depletion in a deep-ocean dissolved inorganic C reservoir that was relatively well isolated from the atmosphere. Renewed ventilation of this reservoir could theoretically explain the drop in atmospheric $\Delta^{14}C$ (Fig. 1C) and the rise in atmospheric CO_2 (*6*) across the last deglaciation. Most workers point to the Southern Ocean as a locus of deglacial CO_2 release, based on the similarity between atmospheric CO_2 and Antarctic temperature records (*6*) and on numerous conceptual and numerical models (*7*–*9*). If correct, we would expect some signature of the low-^{14}C deep-ocean C reservoir to be spread to other basins via Antarctic Intermediate Water (AAIW). Here, we report a strong radiocarbon signal of the deglacial release of old C, recorded in an intermediate-depth sediment core from the northern edge of the eastern tropical North Pacific.

[1]Department of Geological Sciences, University of Colorado, Boulder, CO 80309, USA. [2]Institute of Arctic and Alpine Research, University of Colorado, Boulder, CO 80309, USA. [3]Department of Geology, Kent State University, Kent, OH 44242, USA. [4]Lamont-Doherty Earth Observatory, Columbia University, Palisades, NY 10964, USA.

*These authors contributed equally to this work.
†To whom correspondence should be addressed. E-mail: tom.marchitto@colorado.edu
‡Present address: Environmental Physics, Institute of Biochemistry and Pollutant Dynamics, Eidgenössische Technische Hochschule Zürich, 8092 Zürich, Switzerland.

Intermediate water $\Delta^{14}C$ reconstruction. Marine sediment multi-core/gravity-core/piston-core triplet from sediment layer MV99-MC19/GC31/PC08 was raised from a water depth of 705 m on the open margin off the western coast of southern Baja California (23.5°N, 111.6°W) (*10*). The site is today situated within the regional O_2 minimum zone that exists because of a combination of high export production and poor intermediate-water ventilation. Various sediment properties in MC19/GC31/PC08 vary in concert with the so-called Dansgaard-Oeschger (D-O) cycles that characterized the Northern Hemisphere climate during the last glacial period (*11*). Originally discovered in Greenland ice cores, D-O cycles also exist in a number of lower-latitude locations that were probably teleconnected to the North Atlantic region through the atmosphere (*2*, *12*, *13*). Off the coast of Baja California, the sedimentary concentrations of organic C, Cd, Mo, and benthic foraminifera all decreased sharply during D-O stadials (cold periods in Greenland) (*11*, *14*). Together, these proxies are consistent with reduced productivity during stadials, caused by either decreased coastal upwelling or a deepening of the regional nutricline related to the mean state of the tropical Pacific (*11*).

Diffuse spectral reflectance (DSR) provides a 1-cm resolution stratigraphy for GC31/PC08. After R-mode factor analysis, the third factor of DSR (Fig. 1A) exhibits the strongest correlation to the productivity proxies and to Greenland climate (*11*). We used this DSR record to apply a calendar-age model to MC19/GC31/PC08, based on correlation to $\delta^{18}O$ (an air-temperature proxy) in Greenland ice core GISP2 (Greenland Ice Sheet Project 2) (*15*). Resulting calendar ages were then combined with 50 benthic foraminiferal radiocarbon ages [19 of which were published previously (*10*)] to calculate age-corrected intermediate-water $\Delta^{14}C$ (*16*). To evaluate the partitioning of ^{14}C between the atmosphere and the ocean, we compared intermediate-water $\Delta^{14}C$ to that of the atmosphere (Fig. 1C), as reconstructed from tree rings (*17*), U-Th–dated corals (*1*, *17*), and planktonic foraminifera from Cariaco Basin off Venezuela (*3*). Calendar ages for Cariaco Basin were originally based on the correlation of lithologic climate proxies to the GISP2 $\delta^{18}O$ record (*2*), which has been layer-counted with visual and chemical techniques (*15*). However, Hughen *et al*. (*3*) recently demonstrated that the Cariaco Basin ^{14}C calibration yields much better agreement with coral results older than ~22,000 yr B.P. when an alternate age model is used, based on correlation to the U-Th–dated Hulu Cave speleothem $\delta^{18}O$ record from eastern China (*13*). Because DSR in GC31/PC08 is more similar to the Greenland isotope record than to the lower-resolution Hulu Cave record, we continued to use the GISP2 correlation but applied simple provisional age adjustments to GISP2 older than 23,400 yr B.P., using four tie points to Hulu Cave (Fig. 1B and fig. S1). We do not suggest that this age model is necessarily superior to the original one (*15*), but this exercise is necessary for comparing our data to the most recent (and most consistent) atmospheric $\Delta^{14}C$ reconstructions (*1*, *3*, *17*). The resulting age model for MC19/GC31/PC08, based on 21 tie points, yields a very constant sedimentation rate (fig. S2) and gives us confidence that our calendar-age assignments for ^{14}C samples between tie points are reliable to within a few hundred years (table S1).

Baja California intermediate-water radiocarbon activities are plotted in red in Fig. 1C. The modern activity, based on a local seawater measurement of –131‰ at 445 m and the nearest Geochemical Ocean Section Study profile (*18*), is estimated to be –170‰, in good agreement with the core top value. Comparable offsets from the contemporaneous atmosphere were maintained throughout the Holocene (typically ~100‰ between 0 and 10,000 yr B.P.) and during the latter part of the glacial period (roughly 200‰ between 20,000 and 30,000 yr B.P.) (*19*). Radiocarbon activities before 30,000 yr B.P. show increased scatter that may be related to the greater influence of slight contaminations on older samples.

Overall, it is clear that intermediate waters mainly followed atmospheric $\Delta^{14}C$ over the past 40,000 yr, except during the last deglaciation. Activities dropped sharply just after 18,000 yr B.P., reaching minimum values of ~–180‰ between 15,700 and 14,600 yr B.P., roughly 450‰ lower than that of the contemporaneous atmosphere. For comparison, the lowest $\Delta^{14}C$ values found in the modern ocean (in the North Pacific near 2-km water depth) are depleted by ~240‰, relative to the preindustrial atmosphere (*18*). A second comparably large depletion event began sometime between 13,500 and 12,900 yr B.P. and ended between 12,100 and 11,600 yr B.P. The magnitude of ^{14}C depletion we reconstructed during these two deglacial events is much too great to attribute to changes in dynamics of the North Pacific thermocline (*20*) and must instead record a large change in the initial ^{14}C activity of waters advected to the site. Such depleted waters could have been sourced only from the deepest, most isolated regions of the glacial ocean (*21*).

Link to atmospheric history. In Fig. 2, we compare the timing of reconstructed intermediate-water and atmospheric $\Delta^{14}C$ changes with the deglacial record of atmospheric CO_2 from the East Antarctic Dome C ice core (*6*). The latter is shown on a GISP2 layer-counted time scale based on a simple synchronization of CH_4 variations between the Dome C and GISP2 ice cores (supporting online material text and table S2). It is immediately apparent that the atmospheric $\Delta^{14}C$ decline and CO_2 rise occurred in parallel, with a synchronous, intervening plateau appearing in both records. There is a slight (and still unreconciled) difference in the timing of the start of the deglacial atmospheric $\Delta^{14}C$ decline between the Cariaco Basin (*3*) and IntCal04 (*17*) reconstructions, but we take the deglacial onset of the atmospheric CO_2 rise and the atmospheric ^{14}C decline to be essentially synchronous. We now also find that these changes were associated with a prominent decline in $\Delta^{14}C$ of intermediate water in the eastern North Pacific that must record the redistribution of aged C from the deep ocean to the surface. After 14,600 yr B.P., intermediate-water activities rebounded to higher values, coincident with the plateau in both the atmospheric CO_2 rise and the atmospheric $\Delta^{14}C$ drop. The leveling of the atmospheric records and the increase in ^{14}C activity of intermediate waters are all indicative of a reduction in the flux of aged C to the upper ocean and atmosphere from below. After ~12,800 yr B.P., the atmospheric CO_2 rise and $\Delta^{14}C$ drop resumed, and intermediate-water activities again reached minimum values of ~–180‰, indicating a resumption of C redistribution from the deep ocean to the surface. By 11,500 yr B.P., the large deglacial atmospheric shifts were mostly completed, and intermediate-water activities finally reached modern values.

As pointed out by Monnin *et al.* (*6*), the deglacial rise of atmospheric CO_2 closely followed the rise in East Antarctic temperatures (Fig. 3A), implying that the ocean's release of C to the atmosphere was associated with changes in the Southern Ocean. Deep convection of the Southern Ocean both ventilates much of the ocean interior and returns to the atmosphere much of the C extracted by photosynthesis in the sunlit surface of the global ocean. During the last

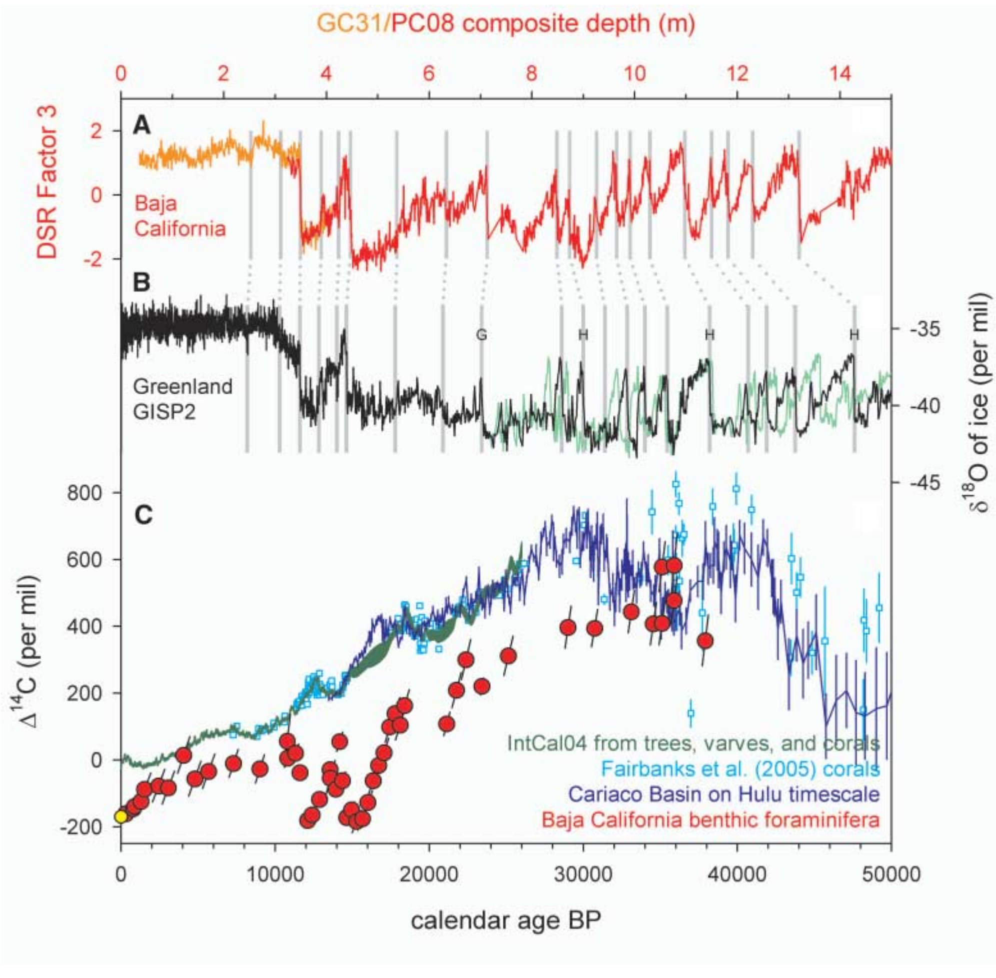

Fig. 1. Intermediate-water and atmospheric $\Delta^{14}C$ records. (**A**) Diffuse spectral reflectance factor 3 from Baja California composite sediment core MV99-GC31/PC08, plotted versus depth (top axis) (*11*). Gray lines show tie points to the Greenland record that were used to derive the calendar-age model. (**B**) $\delta^{18}O$ of Greenland ice core GISP2 (*15*) on a provisional revised time scale (black, bottom axis). The new time scale deviates from the original time scale (green) for calendar ages older than 23,400 yr B.P. (vertical line labeled G). The new time scale is based on linear interpolation between point G and three tie points whose ages are derived from U-Th–dated Hulu Cave (vertical lines labeled H) (*13*). (**C**) Atmospheric radiocarbon activities based on tree rings, planktonic foraminifera from Cariaco Basin varve-counted sediments, and U-Th–dated corals (dark green) (*17*); additional recent coral measurements (light blue) (*1*); and planktonic foraminifera from Cariaco Basin, based on an age model derived from the correlation of sediment reflectance to Hulu Cave (dark blue) (*3*). Red circles show intermediate-water activities from benthic foraminifera in MC19/GC31/PC08. The yellow circle is an estimate for modern bottom waters at this site. Error bars are based on compounded uncertainties in radiocarbon ages and calendar ages.

glacial period, density stratification of the Southern Ocean surface and/or extensive sea-ice coverage are suggested to have isolated deep waters from the atmosphere (*7–9*), permitting the buildup of a larger deep-ocean C reservoir and a consequent drawdown of atmospheric CO_2. Sediment pore water chlorinity and $\delta^{18}O$ measurements, combined with benthic foraminiferal $\delta^{18}O$, indicate that deep Southern Ocean waters were the saltiest and densest waters in the glacial ocean (*22*). Such high salinities point to brine formation beneath sea ice as an important mode of formation. At deglaciation, a progressive renewal of deep convection or upwelling in association with documented sea-ice retreat (*23*) [and possibly with poleward-shifting westerlies (*8*)] would have provided for the simultaneous delivery of ocean heat and sequestered C to the atmosphere. This transition occurred in two major steps, beginning with relatively early (~18,000 years ago) and gradual increases in temperature and CO_2 that were temporarily interrupted by the Antarctic Cold Reversal (ACR). Major transients in our record of $\Delta^{14}C$ in intermediate-depth waters of the eastern North Pacific conform to this Antarctic schedule, consistent with the redistribution of C from the abyss to the upper ocean and atmosphere in connection with changes in deep convection of the Southern Ocean.

$\delta^{13}C$ provides a tracer that is complementary to $\Delta^{14}C$, though with a far smaller dynamic range in seawater. During the last glacial period, the deep Southern Ocean contained the ocean's lowest $\delta^{13}C$ values, suggesting a local accumulation of remineralized C and/or poor ventilation (*24*). Spero and Lea (*25*) argued that during the early part of the last deglaciation, Southern Ocean sea-ice retreat (*23*), combined with increased deep convection and northward Ekman transport, imparted transient low $\delta^{13}C$ values to AAIW and Subantarctic Mode Waters and that this signal was recorded by deep-dwelling planktonic foraminifera in various ocean basins, including the eastern tropical North Pacific. These waters should also have carried a low $\Delta^{14}C$ signature, and we suggest that this is the signal we observe off the coast of Baja California. Today, AAIW is barely traceable as a distinct water mass north of the equator in the eastern tropical Pacific (*26*). We argue that the northward penetration of AAIW during deglaciation was greater than it is today (*27*) and was at times fed by extremely ^{14}C-depleted waters sourced from the abyss by deep overturning in the Southern Ocean. Sea-ice retreat could have allowed the upwelled deep waters to gain buoyancy from precipitation, converting some fraction of these waters into AAIW without substantial mixing with warmer thermocline waters (*28*), which would otherwise dampen the $\Delta^{14}C$ signal. There is evidence that vertical stratification of the North Pacific also varied on an Antarctic climate schedule (*29*), so northern deep waters may have supplemented the supply of aged C to the Baja California site. However, the interaction of strong circumpolar winds with bathymetry in the Southern Ocean provides for much more effective vertical pumping (*30*) than do conditions in the North Pacific, and therefore southern sources probably dominated the $\Delta^{14}C$ changes in our record.

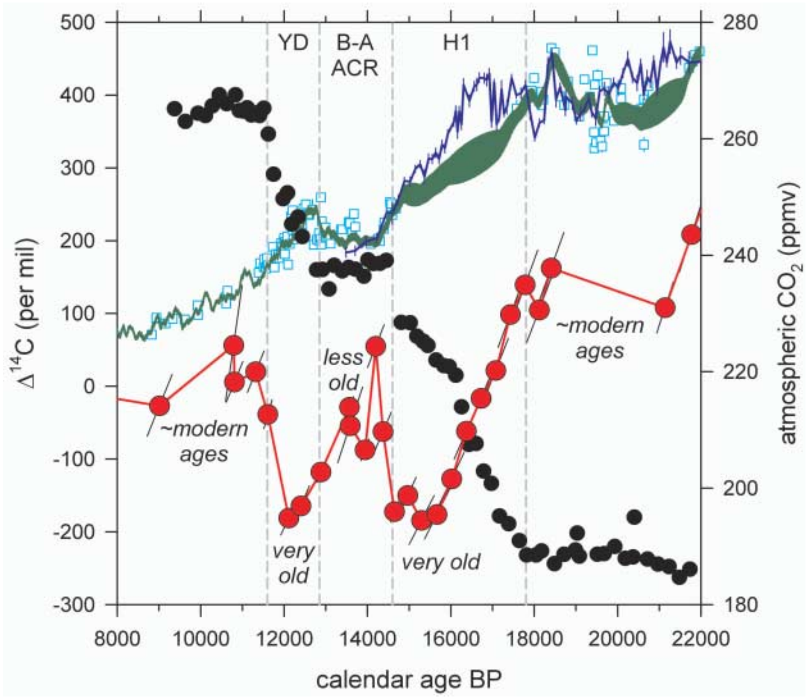

Fig. 2. Baja California intermediate-water $\Delta^{14}C$ during the last deglaciation (red), compared with atmospheric $\Delta^{14}C$ (dark green, light blue, and dark blue) (*1*, *3*, *17*), and atmospheric CO_2 from Antarctica Dome C (*6*) placed on the GISP2 time scale (black), as discussed in the text. Vertical dashed gray lines show the ages of Bølling-Allerød (B-A) and Younger Dryas (YD) boundaries, based on the GISP2 $\delta^{18}O$ record, and the start of Heinrich event 1 (H1), based on the $^{231}Pa/^{230}Th$ record from Bermuda Rise (*34*). The ACR is contemporaneous with the Bølling-Allerød. ppmv, parts per million by volume.

North-south teleconnections. Numerous observational and modeling studies indicate an inverse relationship between Antarctic and North Atlantic temperature variations that may be due to altered interhemispheric ocean-heat transport and/or opposing local deep-water formation histories (*28*, *31–33*). Insofar as $\Delta^{14}C$ of the intermediate-depth Pacific provides an inverse proxy for the strength of deep convection in the Southern Ocean, our results provide strong evidence for tight, inverse coupling of deep-water formation between hemispheres. This is clearly demonstrated by the covariation of intermediate-depth Pacific $\Delta^{14}C$ and the formation history of North Atlantic Deep Water (NADW) [or its glacial analog, Glacial North Atlantic Intermediate Water (GNAIW)], based on measurements of $^{231}Pa/^{230}Th$ from sediments in the western North Atlantic (*34*) (Fig. 3C). The near-cessation of ^{231}Pa export beginning just after 18,000 yr B.P. records a collapse of GNAIW that has been linked to a massive discharge of glacial ice and fresh water to the North Atlantic, known as Heinrich event 1. After a recovery during the Bølling-Allerød warm phase, another marked weakening of NADW/GNAIW is documented during the Younger Dryas cold period, probably also triggered by a discharge of glacial meltwater (*34*). Both periods of NADW/GNAIW reduction were times of intermediate-depth Pacific $\Delta^{14}C$ decline and atmospheric CO_2 rise.

It is often difficult to identify triggers in a tightly coupled system, but the relationships described above suggest that the Antarctic climate schedule may have been paced by ice sheet and meltwater forcing around the North Atlantic. Support for this conclusion comes from our observation that although major inflections in the $\Delta^{14}C$ and $^{231}Pa/^{230}Th$ records in Fig. 3 were almost exactly synchronous, the large $\Delta^{14}C$ decrease (i.e., Southern Ocean ventilation increase) during Heinrich event 1 occurred more gradually than did the associated decrease in GNAIW export. This relationship is consistent with relatively slow circum-Antarctic warming due to anomalous ocean-heat transport (*33*), leading to sea-ice retreat (*23*) [and possibly poleward-shifting westerlies (*8*)] and, consequently, a progressive increase in deep overturning of the Southern Ocean. Alternatively, Southern Ocean overturning may have been instigated by NADW/GNAIW reductions through the requirement (*35*) that global rates of deep-water formation balance global deep upwelling, which is forced mainly by winds and tides. The abrupt rise in atmospheric $\Delta^{14}C$ at the start of the Younger Dryas [+80‰ in just 180 years (*36*)] (Fig. 2) may record the time elapsed before the Southern Ocean could begin respond-

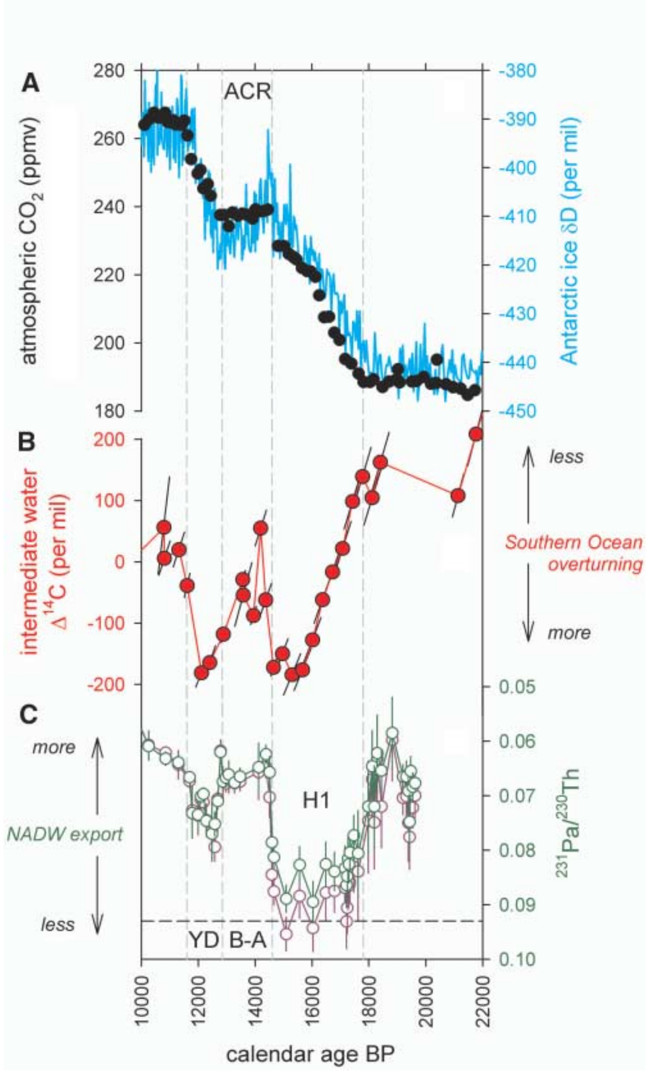

Fig. 3. Southern and northern ocean-atmosphere changes during the last deglaciation, compared with intermediate-water $\Delta^{14}C$. (**A**) Atmospheric CO_2 (black) and ice core deuterium (δD) temperature proxy (light blue) from Antarctica Dome C (*6*), placed on the GISP2 time scale. (**B**) Baja California intermediate-water $\Delta^{14}C$. (**C**) Inverted decay-corrected excess $^{231}Pa/^{230}Th$ in Bermuda Rise sediments, based on two methods to calculate excess (green and purple) (*34*). The horizontal dashed line shows the water-column production ratio for these isotopes (0.093); lower values are primarily due to Pa export by vigorous NADW. Vertical dashed lines show the ages of climatic boundaries, as in Fig. 2. Error bars are based on compound uncertainties in radiocarbon ages and calendar ages.

ing to reduced NADW formation, leading to the brief absence of deep-ocean sinks for ^{14}C (*32*).

Recent work shows that deep North Atlantic radiocarbon activities also increased abruptly during the Bølling-Allerød because of renewed formation of NADW and that they temporarily decreased during the Younger Dryas, when NADW formation was again briefly restricted (*37*, *38*). In light of our new record, this pattern of deep-ocean change was probably limited to the North Atlantic (arising from deep circulation changes within the basin), whereas the intermediate-depth North Pacific record tracks the overall redistribution of C from the deep ocean to the atmosphere.

Implications for the deep C reservoir. Finally, our results bear on recent questions concerning reconstructed rates of atmospheric $\Delta^{14}C$ decline during deglaciation and implied ^{14}C aging of glacial deep waters. Although subject to uncertainties (*19*), decay projection of our first deglacial $\Delta^{14}C$ minimum back to the surface ocean (*39*) gives an apparent ventilation age of ~4000 years, implying that the inferred deep Southern Ocean source waters were at least that old. This is broadly consistent with the minimum deep-ocean age estimated from the atmospheric record, assuming that the old reservoir filled half of the ocean's volume (*40*). Ages of up to 5000 years have been reported for glacial deep waters near New Zealand (*41*), but more northerly sites in the Pacific show little difference from today, at least at depths shallower than ~2 km (*40*). We infer that the greatest ^{14}C depletion of the glacial deep ocean was probably concentrated in the Southern Ocean region (and deepest Pacific), coincident with the highest densities (*22*) and lowest $\delta^{13}C$ values (*24*).

References and Notes

1. R. G. Fairbanks *et al.*, *Quat. Sci. Rev.* **24**, 1781 (2005).
2. K. Hughen *et al.*, *Science* **303**, 202 (2004).
3. K. Hughen, J. Southon, S. J. Lehman, C. Bertrand, J. Turnbull, *Quat. Sci. Rev.* **25**, 3216 (2006).
4. C. Laj *et al.*, *Earth Planet. Sci. Lett.* **200**, 177 (2002).
5. R. Muscheler *et al.*, *Earth Planet. Sci. Lett.* **219**, 325 (2004).
6. E. Monnin *et al.*, *Science* **291**, 112 (2001).
7. D. M. Sigman, E. A. Boyle, *Nature* **407**, 859 (2000).
8. J. R. Toggweiler, J. L. Russell, S. R. Carson, *Paleoceanography* **21**, PA2005 (2006).
9. B. B. Stephens, R. F. Keeling, *Nature* **404**, 171 (2000).
10. A. van Geen *et al.*, *Paleoceanography* **18**, 1098 (2003).
11. J. D. Ortiz *et al.*, *Geology* **32**, 521 (2004).
12. R. J. Behl, J. P. Kennett, *Nature* **379**, 243 (1996).
13. Y. J. Wang *et al.*, *Science* **294**, 2345 (2001).
14. W. E. Dean, Y. Zheng, J. D. Ortiz, A. van Geen, *Paleoceanography* **21**, PA4209 (2006).
15. P. M. Grootes, M. Stuiver, *J. Geophys. Res.* **102**, 26455 (1997).
16. Materials and methods are available as supporting material on *Science* Online. In the supporting material, we also present our $\Delta^{14}C$ values calculated with the original GISP2 chronology (*15*) and compare them to the original Cariaco record (*2*), based on correlation to GISP2 (fig. S3).
17. P. J. Reimer *et al.*, *Radiocarbon* **46**, 1029 (2004).
18. G. Ostlund, H. Craig, W. S. Broecker, D. Spencer, *GEOSECS Atlantic, Pacific and Indian Ocean Expeditions*, vol. 7, *Shorebased Data and Graphics* (U.S. Government Printing Office, Washington, DC, 1987).
19. Throughout most of this paper, we discuss our $\Delta^{14}C$ values with respect to the contemporaneous atmosphere, rather than calculating ventilation ages by decay projection (*39*) because of large uncertainties in initial surface-ocean reservoir ages and the possibility of multiple intermediate- and deep-water sources with different ventilation histories.
20. U. Mikolajewicz, T. J. Crowley, A. Schiller, R. Voss, *Nature* **387**, 384 (1997).
21. The deglacial injection of low-^{14}C intermediate waters along the Baja California margin did not noticeably overprint the DSR or other O_2-sensitive productivity proxies recorded in GC31/PC08. Although $\Delta^{14}C$ and O_2 are broadly correlated in the modern ocean, they can also be decoupled (*18*) through air-sea exchange. Hence, deglacial intermediate waters were very depleted in $\Delta^{14}C$ but apparently not drastically depleted in O_2.
22. J. F. Adkins, K. McIntyre, D. P. Schrag, *Science* **298**, 1769 (2002).
23. R. Gersonde, X. Crosta, A. Abelmann, L. Armand, *Quat. Sci. Rev.* **24**, 869 (2005).
24. U. S. Ninnemann, C. D. Charles, *Earth Planet. Sci. Lett.* **201**, 383 (2002).
25. H. J. Spero, D. W. Lea, *Science* **296**, 522 (2002).
26. P. C. Fiedler, L. D. Talley, *Prog. Oceanogr.* **69**, 143 (2006).
27. S. Schulte, F. Rostek, E. Bard, J. Rullkötter, O. Marchal, *Earth Planet. Sci. Lett.* **173**, 205 (1999).
28. R. F. Keeling, B. B. Stephens, *Paleoceanography* **16**, 112 (2001).
29. S. L. Jaccard *et al.*, *Science* **308**, 1003 (2005).
30. J. R. Toggweiler, B. Samuels, *Deep-Sea Res.* **42**, 477 (1995).
31. T. J. Crowley, *Paleoceanography* **7**, 489 (1992).
32. W. S. Broecker, *Paleoceanography* **13**, 119 (1998).
33. R. Knutti, J. Flückiger, T. F. Stocker, A. Timmermann, *Nature* **430**, 851 (2004).
34. J. F. McManus, R. Francois, J.-M. Gherardi, L. D. Keigwin, S. Brown-Leger, *Nature* **428**, 834 (2004).
35. W. Munk, C. Wunsch, *Deep-Sea Res.* **45**, 1977 (1998).
36. K. A. Hughen, J. R. Southon, S. J. Lehman, J. T. Overpeck, *Science* **290**, 1951 (2000).
37. L. C. Skinner, N. J. Shackleton, *Paleoceanography* **19**, PA2005 (2004).
38. L. F. Robinson *et al.*, *Science* **310**, 1469 (2005).
39. J. F. Adkins, E. A. Boyle, *Paleoceanography* **12**, 337 (1997).
40. W. Broecker *et al.*, *Science* **306**, 1169 (2004).
41. E. L. Sikes, C. R. Samson, T. P. Guilderson, W. R. Howard, *Nature* **405**, 555 (2000).
42. We thank D. Lopez, J. Turnbull, and C. Wolak for laboratory assistance; J. Southon for accelerator mass spectrometry analyses; A. Pearson for providing an unpublished seawater $\Delta^{14}C$ measurement; and T. Blunier for providing Dome C EDC 3 time scale and for valuable discussions on synchronization of the different ice cores. This manuscript was improved by comments from R. Keeling and two anonymous reviewers. Support was provided by NSF grants OCE-9809026 and OCE-0214221.

Supporting Online Material

www.sciencemag.org/cgi/content/full/1138679/DC1
Materials and Methods
SOM Text
Figs. S1 to S3
Tables S1 and S2
References

11 December 2006; accepted 27 April 2007
Published online 10 May 2007;
10.1126/science.1138679
Include this information when citing this paper.